Estuaries Vol. 25, No. 2, p. 204–214 April 2002

The Impact of Mobile Disarticulated Shells of *Cerastoderma edulis* on the Abrasion of a Cohesive Substrate

C. E. L. THOMPSON* AND C. L. AMOS

Southampton Oceanography Centre, University of Southampton, European Way, Southampton, SO14 3ZH, United Kingdom

ABSTRACT: An annular laboratory flume was used to investigate the effect of mobile cockle shells on the erosion of a cohesive sediment bed. A standard clay bed was created and shells of differing sizes placed upon it. Flow in the flume was increased in increments and the onset of motion and the transport patterns of the cockles were monitored. The release of bed material to the water column was monitored and compared to controls made in the absence of shells (due only to the flow). The shells moved as bedload; first as surface creep (sliding) and then by rolling. The onset velocity of motion (U_c) of the shells was found to be directly related to the settling rate (W_s) in still water. The fluid-induced stresses did not cause any detectable erosion of the bed. The addition of even a single shell induced significant erosion rates (E). The erosion was found to be the result of abrasion rather than corrasion, as the shells never entered into saltation. There was a linear increase in erosion rate with increasing shell size, and an exponential increase in the suspended sediment concentration with time. The drag coefficients (C_d) for settling in traction were calculated. The ratio of the drag forces acting on the shells when settling and moving as traction was found to equal to $1/\tan(\phi)$ where ϕ is the friction angle.

Introduction

The tidal flats and salt marshes of the south coast of England are rapidly retreating (Riddell and Ishaq 1994) yet there appears to be no physical explanation for much of the observed retreat. These flats are littered with disarticulated shells of the edible cockle *Cerastoderma edulis,* which appear to be concentrated in areas of strong erosion, such as at the foot of eroding marsh cliffs (Fig. 1).

It has been postulated that abrasion due to the motion of *C. edulis* shells is responsible for the formation and maintenance of mud furrows in Southampton Water (Dyer 1970). The erosion of salt marshes at Hythe, Hampshire appears to be taking place in regions infested by mobile banks of *C. edulis.* Work in Southampton has revealed a series of V-shaped furrows up to 5 cm wide and up to 1 m deep. The furrows seem to quickly re-establish after dredging, and their length, regularity, and continuity suggests they are of natural origin and not the product of dredging (Dyer 1970).

Previous studies have shown the importance of abrasion of coastal bluffs caused by the movement of sand, gravel, and other materials (Bishop et al. 1992; Skafel and Bishop 1994; Skafel 1995), but have not provided a means of quantifying it (Davidson-Arnott and Ollerheads 1995). The evolution of some beds has been suggested to be controlled by the physical properties of the mobile aggregate and almost independent of the cohesive substrate (Kamphuis 1990).

The principle of abrasion has recently been used by the UK Ministry of Defence in the production of abrasive cutting equipment for the aid of bomb disposal. It works by combining water and sand, and delivering them through a small nozzle at high pressures (Louis and Pude 2000). This erodes the metal surface of the bomb, eliminating the need for cutting, and works using the same principles as the impact of grains on a sediment bed promoting erosion of that bed. It has also been used in etching glass, wood, metal, and plastics, in cleaning machinery and in shot basting, which produces a smooth finish on machinery. A new technique called air abrasion has also been created for dentistry, using 2.75 micron aluminium oxide powder administered under compressed air through a very fine tip to eliminate the need for drills (Wright et al. 1999). The understanding of the basic process of abrasion in the coastal zone may help advance the use of this technology for other purposes.

The erosion and transport of sediments in the marine environment is largely explained and modeled in terms of the prevalent hydrodynamics in the form of a fluid-transmitted shear stress to the bed. Bagnold (1936) observed that some of the energy needed for sand transport is provided by the motion of the sand itself in the form of a solid-transmitted stress. Allen (1971) has shown that the transport of coarse material over a muddy bed can cause scouring and the formation of bed features

* Corresponding author; tele: 44(0)23 80596574; fax: 44(0)23 80593642; e-mail: celt1@soc.soton.ac.uk.

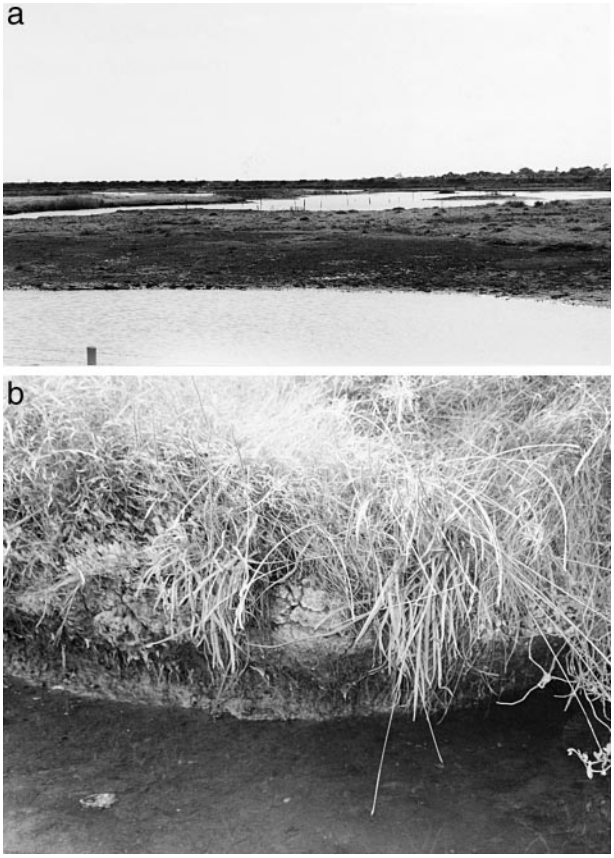

Fig. 1. Images of the salt marshes in Lymington, South Coast of England. Top panel: panoramic view of the salt marshes and seaward eroding bluff. Bottom panel: the undercut eroding bluff, which typifies most salt marshes of southern England.

such as tool marks. Amos et al. (2000) has shown that saltating littorinid shells can greatly increase erosion of a cohesive bed through the effect of the solid-transmitted stress in a manner described as the ballistic momentum flux (BMF). The imprints of the motion of mobile aggregates moving as bedload over cohesive beds are physical manifestations of scour through the BMF (Rice et al. 1996). This process is termed corrasion (see Allen 1985 for review). We propose that this mechanism is at work in the nearshore of southern England.

Several areas in the south of Britain and Europe have been identified as having tool marks similar to those caused by corrasion, and the presence of shell material is found in many of them. Enhanced scour through corrasion can amplify the release of nutrients and pollutants as well as sediments into the water column and eventually the food chain (Levy 2000). This investigation hopes to identify the extent to which cockle shells increase the erosion of a cohesive bed through corrasion and hopes to quantify the process.

General Background

The erosion of cohesive beds is largely considered to be a continuous process of particle release into suspension when the shear stress is above some threshold (Houwing 1999). Erosion can be complicated by the addition of a saltation load and a traction load, which often occur over mudflats (Amos et al. 1992). A solid transmitted shear stress is imparted to the bed from the motion of the saltating particles (Bagnold 1936; Bitter 1963).

Cohesive sediment particle movement is controlled not only by internal, gravitational, buoyancy, and drag forces, but also by electrochemical ones due to their small size (Scarlatos and Mehta 1990). Under certain conditions the forces become attractive and occur at the points of contact between the individual particles (Partheniades 1986). The strength of a cohesive sediment bed is often expressed in terms of the critical shear stress for erosion (τ_c) and the erosion rate (E). The critical erosion threshold is the moment at which bed sediments are entrained into suspension by the fluid flow (Houwing 1999) although there is much debate about its significance and definition (Sutherland et al. 1998). This moment of erosion will be determined by the composition of the bed, the bed density, and biological activity in the topmost layer of the bed (the biofilm). τ_c is some function of the shear strength, clay content, and other basic geotechnical properties of the cohesive material (Davidson-Arnott and Ollerheads 1995). In nature, the properties of cohesive sediments are significantly affected by chemical and biological factors; clay particles absorb pollutants, especially heavy metals and pesticides (Mehta and Dyer 1990). Bioturbation acts both to increase cohesiveness and to loosen beds and resuspend sediment (Mehta and Dyer 1990). Because of these factors, the erosion threshold and erosion rates of cohesive beds are difficult to predict (Amos et al. 1992).

When water transports material of a density greater than itself, the material motion may be confined to a thin zone within a few diameters above the bed. They either roll along the bed (traction) or saltate in a series of low jumps (saltation). The contribution of traction and saltation is termed bedload (Bagnold 1936). The motion of the material can be classified as bedload if the bed supports it either continuously or intermittently. The sediment is considered to move in suspension if the particles hit the bed so infrequently that the particles net weight is supported by the fluid rather than the bed (Murphy et al. 1985). The bedload component has been found to be capable of influencing the benthic flux of sediment through erosion of cohesive mudflats in the Annapolis Basin,

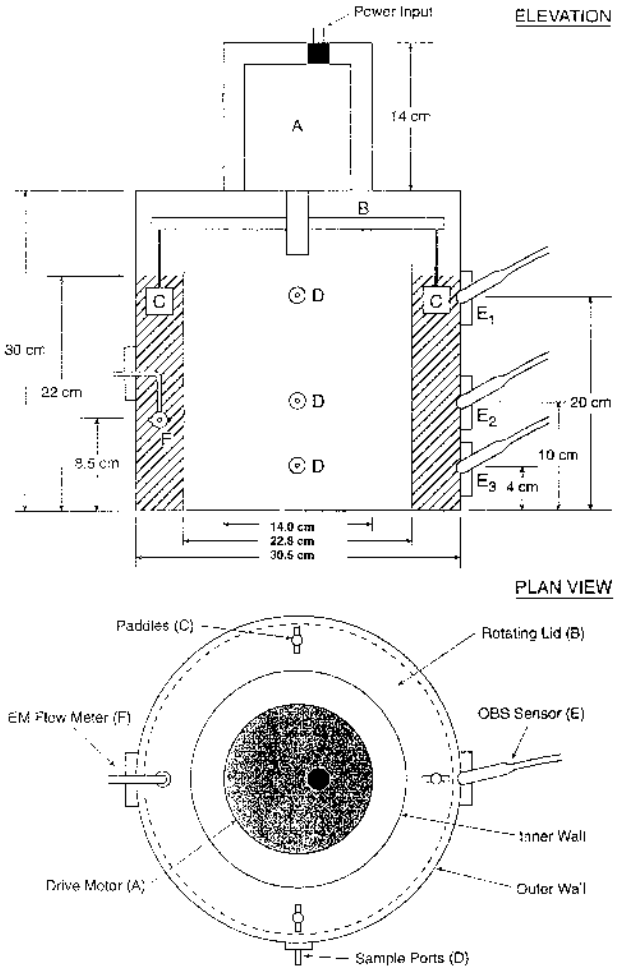

Fig. 2. A schematic diagram of the Mini Flume.

Bay of Fundy, Canada (Amos et al. 1992). Flowing water has the effect of enhancing wear through momentum transfer (both fluid and solid transmitted), while dampening it through the role of lubrication at the contact point of colliding solid objects (Granick 1999). The total shear stress (τ_{tot}) is the combination of the fluid-transmitted stress (τ_o) and the BMF (T): $\tau_{tot} = \tau_o + T$. It is T which results in abrasion and corrasion of a cohesive bed, and which has largely been ignored in studies of bed stability in sub-aqueous settings.

Methods

The Mini Flume

The Mini Flume is a benthic annular flume consisting of two acrylic tubes sitting inside one another to form a channel 4.5 cm wide and 22 cm high (Fig. 2), and an open base. The tubes are injected into a prepared clay bed to create a sealed flume (Amos et al. 2000). A rotating lid creates a current using four square paddles spaced equidistantly. The paddle speed is controlled by a Compumotor digital DC stepping motor, powered by a 24 bit DC, 1000 watt power supply. The motor is controlled by a PC connected to it through a RS232 serial link. An ASCII script file is used to control the motor controller that, in turn, controls the speed, duration, and acceleration of the rotating lid. Lid rotation is reproducible and consistent. Currents in the horizontal and vertical directions are measured using a Marsh-McBirney model 513 electro-magnetic current meter (EMCM) situated at a height of 8.5 cm above the base. Three D & A Instruments optical backscatter sensors (OBS) measure turbidity at 4, 10, and 20 cm above the base, and are in line with three sample ports used for sensor calibration. The data from the EMCM and the three OBS were logged to a CR10 data logger at a rate of 1 Hz.

Three-dimensional flow measurements within the Mini Flume were made using a Laser Doppler Velocimeter (Fung 1997). These measurements showed a well-developed boundary layer about 10 mm thick, a natural turbulent structure within the boundary layer, and a weak 3-dimensional circulation. Above the boundary layer, the mean azimuthal velocity is constant with height (Amos et al. 2000). No evidence was found in near-bed energy spectra of peaks at paddle or lid frequencies (Fung 1997). Johansen et al. (1997) found that in a stationary circular flume with a rotating lid the velocity increases across the flume from the inner wall to the outer wall due to secondary circulation and decreases from the top to the bottom affecting the vertical distribution of suspended sediment. These secondary currents have been accounted for in the evaluation of the bed shear stress.

Bed Preparation

The beds used in this study were prepared from a standard non-grog white potter's clay with a 20% water content. Remolded clay was used in order to eliminate the complexities of consolidation time, inevitable when using a settled bed, or disturbances to natural sediments caused by transporting them and placing them in the flume (Sutherland et al. 1998). A bed of uniform properties was created that could be easily reproduced; enabling experimental procedures to be standardized. White clay was chosen because it reflected a larger proportion of light than natural (red/brown) clay, resulting in greater sensitivity of the OBS (Sutherland et al. 1998). The plasticity and density of the clay was such that it was easily remolded; yet still maintained a good seal around the base of the flume.

Houwing and van Rijn (1994) found that if variation in sand-mud composition, bed density, grain

size distribution, and biological activity is relatively small, the strength of the top layer of cohesive beds at different locations tends to be constant. Therefore it can be assumed that the behavior of the cohesive bed used for this investigation will not be changed by slight variations in the clay (all the clay was from the same batch) or by rolling of the sample bed. Three replicates were carried out for each size class to evaluate experimental error.

A uniform bed just larger than the base of the Mini Flume was rolled to a thickness of 2–5 cm. The tubes of the Mini Flume were then pressed into this bed and the clay sealed around them, ensuring the volume of the flume above the bed was the same for each experiment. The friction angle was determined by placing the cockle shells on a piece of rolled clay on a tilting board submerged in water. The friction angle is defined as the angle of tilt at which the shell begins to slide.

The Experiment

The flume was filled with freshwater at room temperature (24°C) to a height of 22 cm. Shell motion was video-taped for the duration of each experiment. A 10-min period of still-stand was recorded initially, followed by 8 increments of constant flow speed; each of a duration of 10 min. Sediment samples were taken 5 min into each speed increment to calibrate the three OBS. Sixty ml of water was drawn off from the center sample and filtered through pre-weighed Whatman GCS glass microfiber filters (24 mm in diameter). They were then dried for 24 h, desiccated and reweighed, and the suspended sediment concentration determined gravimetrically. The lid velocity was calibrated by timing the lid rotation at each velocity step. The raw data was processed using a program that performed the following functions: defines the fluid standard values of viscosity (kg ms^{-1}) and clear water unit weight of freshwater at 24°C (kg m^{-3}); reads the source file from the logger: 3 OBS channels, vertical velocity, horizontal velocity, time code from logger; and using user defined calibrations, calculates the values of suspended sediment concentration (mg l^{-1}), current velocity (m s^{-1}), and erosion rate (kg m^{-2} s^{-1}). The EMCM was calibrated prior to use in a tow tank at the Bedford Institute of Oceanography. All calibrations were linear over the range of measurements.

Shell Description

The shells used have been identified according to Tebble (1966) as *C. edulis* (Linnaeus), the edible cockle. The shells can reach up to 51 mm in length. They are sculptured with 22–28 radiating ribs, each with numerous scale-like spines and very irregular concentric lines. The growth stages are prominent so their age can be determined. This cockle species tends to inhabit clean sand, muddy sand, mud, or muddy gravel, burrowing to a depth no greater than approximately 50 cm (Tebble 1966). It inhabits the area between mid-tide level and low water level and is commonly found in sandy bays, rivers, and estuaries in the British Isles. The specimens used in this investigation were all disarticulated as these were the most common type found in the collection area (Lymington, UK). The shells range in size from 8–39 mm in length (measured along the longest axis), and were representative of the typical range of sizes present in the Lymington area.

TABLE 1. Shell attributes: maximum size diameter (d_{max}), average settling velocity (W_s), and average sedimentation diameter (d_s).

Size Group	d_{max} (mm)	W_s (m s^{-1})	d_s (mm)
1	11	0.31	1.33
2	17	0.39	1.4
3	20	0.48	1.1
4	24	0.51	1.6
5	30	0.56	1.78
6	37	0.55	1.73

Each shell was prepared by cleaning it in dilute hydrogen peroxide to remove all organic material; any damaged specimens were discarded. The shells were numbered and the population divided into 6 provisional size classes: 8–13, 14–18, 19–22, 13–26, 27–33, and $>$ 33 mm. Each shell was weighed dry and the approximate density (ρ_s) of the shell material was determined. This was done by first measuring the volume by submersion of the shells in water and measurement of the water displaced. The density was found to be 2,600 kg m^{-3}, which corresponds well with the value of 2,650 kg m^{-3} normally used for calcium carbonate material. The purpose of the settling experiment was to determine the hydrodynamic behavior of disarticulated shells, and to determine an equivalent sedimentation diameter that could be used to predict the onset of motion as well as the mode of transport of the shell material.

Results

Settling Experiments

The settling velocity and trajectory of the shells were measured by timing their fall in a still column of freshwater 2 m in height. Each shell was settled individually, and three replicates were performed for each shell (Table 1). The shell valves were found to settle always in the convex down attitude. Figure 3a is a schematic representation of the forces acting on a shell immersed in a fluid flow on a flat bed (modified after Swamee and Ojha 1991).

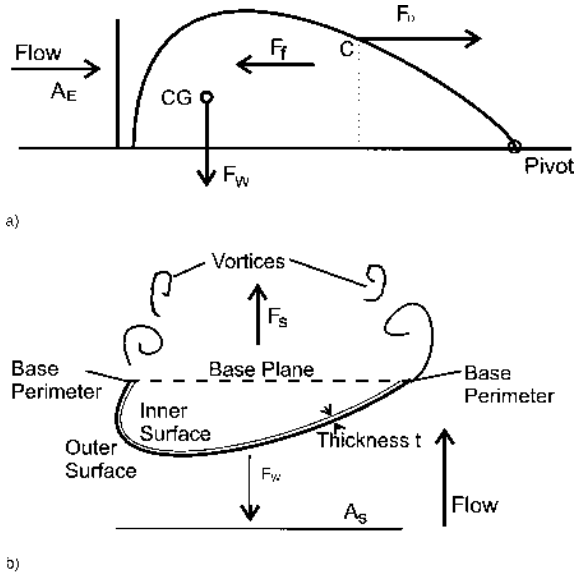

F_D = drag force

F_F – friction

CG = centre of gravity

F_w = immersed weight

A_E, A_s – area of interaction with the flow: eroding and settling respectively

F_s – force acting on a shell as it settles through still water

Fig. 3. The balance of forces acting upon a disarticulated cockle shell (modified after Swamee and Ojha 1991): a) sitting convex up on a flat bed and b) settling convex down in still water.

F_D is the drag force due to the fluid, F_W is the immersed weight, F_F is the friction drag force with the bed, C_G is the center of gravity, C is the point of drag action, and A_E is the area acted upon by the flow (Olivera and Wood 1997). Figure 3b is a schematic representation of the forces acting on a shell settling in still water. F_W is the immersed weight, F_s is the fluid drag force acting on the settling shell, and A_S is the area acted upon by the flow (Mehta et al. 1980). Mehta et al. (1980) identified two modes of settling: stable, where the hydrodynamic pressure and the shear forces are balanced and the shells fall primarily in a downward motion along the fall centerline; and unstable, where sliding and tipping are pronounced with the shell falling in curved descending arcs. Both modes of settling were noted during the settling experiments, however the unstable mode was more common. The Reynolds number ($Re = W_s d_{max}/\nu$ where W_s is the settling velocity, d_{max} is the maximum shell length, and ν is the kinematic viscosity of freshwater) of each shell was plotted against I = 1 − (intermediate length/longest length), for comparison with the work of Allen (1985) on the settling of bivalve shells. Allen describes a critical value of I = 0.4 separating the two modes of transport—any value below this indicates stable settling. It was found that the shells in this study fell below the critical value. When the data were compared with work by Willmarth et al. (1964) and Stringham et al. (1969) on the settling of solitary discs, the shells were found to fall within the zone termed as tumbling or oscillating; that is unstable settling. The Reynolds number has been found to be nearly independent of the drag coefficient (C_d) for settling bivalve shells (Mehta et al. 1980) and so initially a single drag coefficient $C_d = 1$ was used to calculate the drag force of a fluid on the shell in keeping with Mehta's calculations for unstable settling. This was re-evaluated during the course of this study.

Equivalent Sedimentation Diameter

The classification of shells into different sizes may have no hydrodynamic significance because of the variations of roughness, density, and shape of the shells, which control settling rate, and which may differ with growth stage (Amos et al. 2000). The settling velocity and sedimentation diameter determine the onset of shell motion and the way a shell is transported. The sedimentation diameter (D_S) was initially determined according to Swamee and Ojha (1991) for spheres (Table 1):

$$D_s = \frac{3W_s^2 C_{ds}}{4g(s-1)} \quad (1)$$

where s is the relative density of the particle, and C_{ds} is the drag coefficient during settling.

Balance of Forces Acting on a Shell

The forces acting on the shell while settling at terminal velocity (W_s) in still water (F_s) was calculated from the relationship:

$$F_s = A_s \rho C_{ds} W_s^2 = mg = (\rho_s - \rho)Vg \quad (2)$$

$$C_{ds} = \frac{(\rho_s - \rho)Vg}{A_s \rho W_s^2} \quad (3)$$

where ρ is the freshwater density, and V is the shell solid volume. A_s is the area the drag force acts upon while settling, and ρ_s is the density of the shell material. C_{ds} may be calculated as it is the only unknown in Eq. 3.

The forces acting on the shell at the point of motion while sitting on the bed (F_D) was calculated using the formula:

TABLE 2. Shell drag coefficients and friction angles.

C_{ds}	C_d	ϕ	F_S/F_D	$1/\tan(\phi)$
0.175376	0.097177	44.1458	1.030271	1.030271
0.159623	0.118982	46.6541	0.943866	0.943866
0.206036	0.186526	50.8346	0.814575	0.814575
0.214437	0.166673	51.6707	0.790583	0.790583
0.196807	0.15115	51.6707	0.790583	0.790583
0.24751	0.227571	54.179	0.72178	0.72178
0.277782	0.219117	54.179	0.72178	0.72178
0.260502	0.184155	54.179	0.72178	0.72178
0.245667	0.252221	56.6873	0.657195	0.657195
0.335952	0.223622	47.5234	0.636496	0.636496
0.456118	0.492815	61.7039	0.538357	0.538357
0.347447	0.500878	62.54	0.51968	0.51968
0.399512	0.254942	62.54	0.51968	0.51968
0.501485	0.529099	66.7205	0.430244	0.430244
0.433948	0.516824	66.7205	0.430244	0.430244

$$F_D = A_E\tau_c = (\rho_s - \rho)Vg \times \tan\phi, \quad \text{where } \tau_c = C_d\rho U_{8.5}^2 \tag{4}$$

$$C_d = \frac{(\rho_s - \rho)Vg \tan\phi}{A_c\rho U_{8.5}^2} \tag{5}$$

$$\frac{C_d}{C_{ds}} = \left(\frac{W_s}{U_{8.5}}\right)^2 \frac{A_s}{A_c \tan\phi} \tag{6}$$

where A_E is the area of the shell that the force acts upon, $U_{8.5}$ is the velocity at a height of 8.5 cm above the bed (the height of the EMCM), ϕ is the friction angle between the shell and the bed, and τ_c is the critical shear stress for shell traction. The forces of drag were compared in order to investigate the factors which induce a shell to move in traction as bedload ($\tan(\phi)$, A_e) and those that act on a shell as it settles through water (A_s). The ratio of these forces is proportional to the friction angle as follows:

$$\frac{F_s}{F_D} = \frac{A_s W_s^2 C_{ds}}{A_E U_{8.5}^2 C_d} = \frac{1}{\tan(\phi)} \tag{7}$$

Table 2 shows the calculated values of C_d, C_{ds}, ϕ, F_s/F_d, and $\tan\phi$. As can be seen in Fig. 4, the relationship predicted by Eq. 7 is satisfied. The ratio F_s/F_d is a function of relative area, relative velocity and drag, and inversely related to the measured $\tan(\phi)$ in the linear form:

$$\frac{F_s}{F_D} = 1.02\left(\frac{1}{\tan\phi}\right), \quad r^2 = 0.99; \quad p = 0.01 \tag{8}$$

Note that C_{ds} is not constant, and varies between 0.16 and 0.50 in proportion with C_d; the consequence of varying shell shapes (Mehta et al. 1980; Dyer 1986).

The grain Reynolds number for cockle shells is much greater than 400, confirming that settling takes place within the impact (turbulent) range. This is backed up by a strong linear relationship between the settling velocity and the square root of the maximum shell diameter as can be seen in Fig. 5.

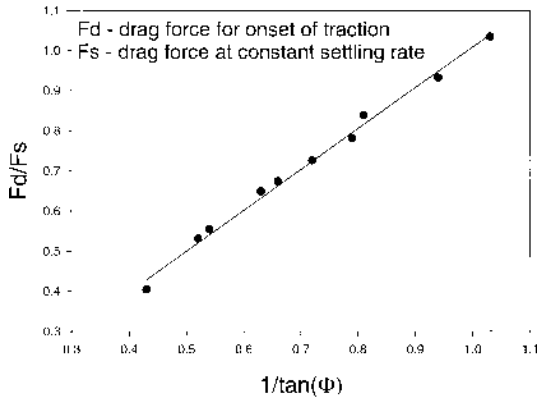

Fig. 4. The ratio of the drag force during settling (F_S) and the drag force during traction (F_D) plotted against $1/\tan(\phi)$. The relationship is linear and close to unity.

Bed Properties

A total of 20 experiments were carried out in this study. The first set was used to determine the parameters required for the motor control program, an ASCII script file used to control the speed and acceleration of the lid rotation used in each experiment. The second set of experiments was carried out without shells in order to establish the fluid-induced erosion of the bed. The final set was undertaken to examine the effects of single shells of different sizes on bed erosion.

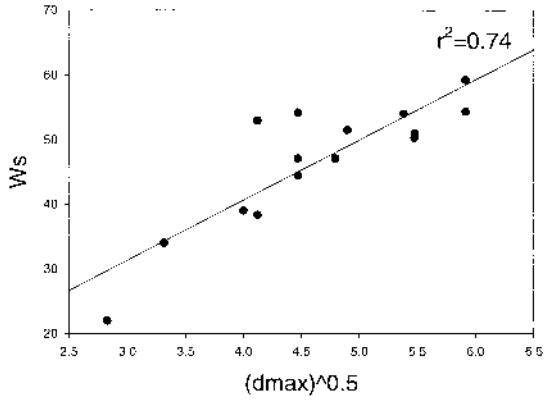

W_s = settling velocity

D_{max} = maximum diameter of shell

Fig. 5. The relationship between settling velocity (W_S) and maximum shell length (D_{max}).

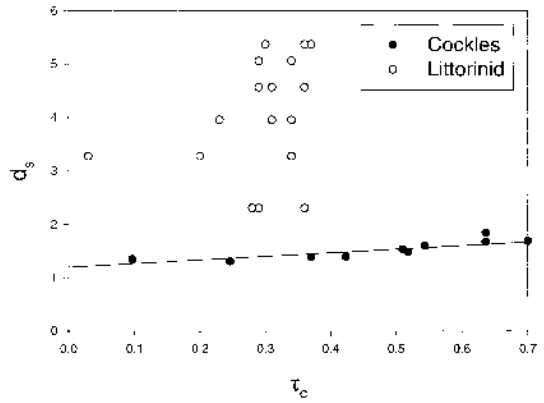

d_s = sedimentation diameter

τ_0 = shear stress at shell motion

Fig. 6. The relationship between sedimentation diameter (D_s) and the bed shear stress for initiation of motion for a) disarticulated cockle shells and b) littorinids.

The experiment to determine the fluid-induced erosion concluded that, under the velocities used for the experiment (which reached in excess of 1 m s^{-1}), no erosion of the standard bed took place due to fluid motion alone. Therefore all the erosion noted in later experiments is purely the result of shell motion.

Shell Behavior

Shells added to the still water of the Mini Flume settled convex down as noted in the settling experiments. Upon the onset of flow (immediately the paddles began to turn), the shells flipped over to sit convex up on the bed until the start of shell motion. Once in motion, the shells continued to travel convex up. They never saltated, but remained in constant contact with the bed. Nor did they roll, but instead skidded or slid across the bed.

Figure 6 shows the linear relationship between the sedimentation diameter and the fluid-transmitted bed shear stress for shell motion: $d_s = 0.94\tau_c + 1.22$, $r^2 = 0.70$. This relationship is weaker than that shown in Fig. 4 and indicates that sedimentation diameter is only a weak proxy of shell stability for the reasons given above.

The Effect of Shell Motion on Bed Erosion

Erosion of the bed began at the onset of shell motion. This can be seen in Fig. 7, where the suspended sediment concentration only begins to increase once the shell moves. Visible tracks (tool marks) were left in the bed as a consequence of shell motion. An exponential increase in the suspended sediment concentration with time and a linear increase in the erosion rate was found. The

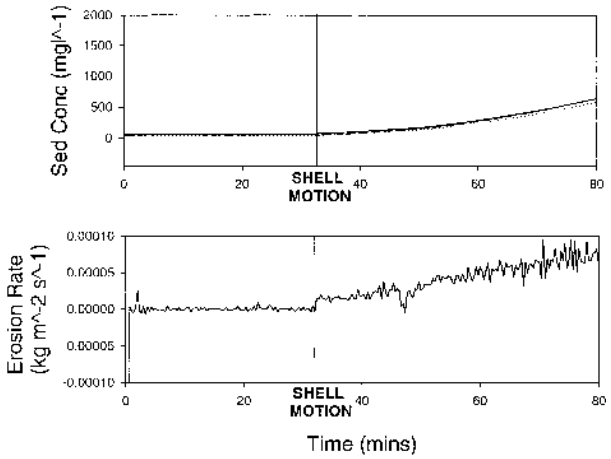

Fig. 7. Time series plots of a) suspended sediment concentration and b) erosion rate at the onset of shell motion. Note turbidity increases abruptly when the shell begins to move.

erosion rate and the maximum suspended sediment concentration increased with shell size. In order to properly investigate the effect of shell size on erosion, the erosion thresholds (or critical shear stresses; Houwing 1999) were calculated.

The fluid-transmitted bed shear stress was calculated from the relationship:

$$\tau = \rho U_*^2 \quad (9)$$

where $U_* = 0.141U_{8.5}$, and the critical shear stress for erosion was determined by extrapolating to zero concentration the line of best fit from plots of the suspended sediment concentration against shear stress. There is a strong correlation between these two shear stresses of the form ($r^2 = 0.81$; Fig. 8):

$$\tau_c = 1.21\tau_0 + 0.04 \quad (10)$$

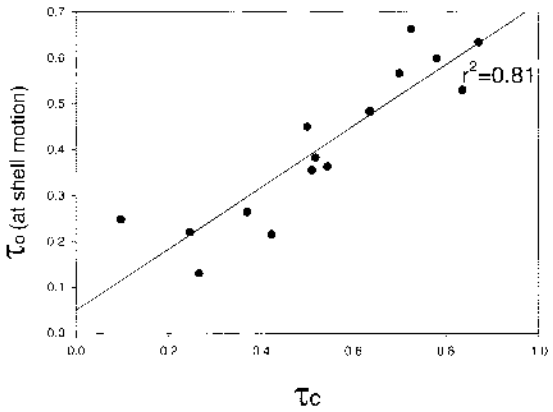

Fig. 8. The relationship between applied bed shear stress and the critical shear stress for bed erosion. Note the relationship is close to unity indicating that erosion is governed by the shell mobility rather than by sediment properties.

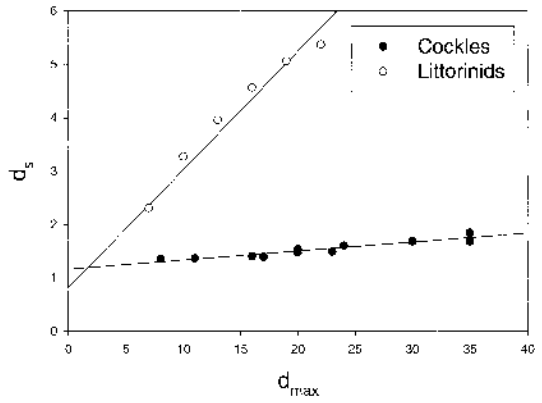

Fig. 9. The relationship between sedimentation diameter and maximum shell length of a) cockles and b) littorinids. Note the large difference between the two shell types, especially at high sedimentation rates.

The relationship is close to unity, which would indicate that the bed erosion threshold is governed by the onset of motion of the shells.

The mean shell motion (U_g) was 56% of the near-bed flow. The difference in speed between the shells and the nearbed flow is due to the momentum dissipated to the bed by the shells. Thus the momentum loss is 44%, which is about 10% higher than the value estimated by Amos et al. (2000) for saltating littorinids. This may be due to the increased periods in which the cockle valves were in contact with the bed, or it may be due to geometrical differences between the two shell types.

Discussion

Shell Responses

Figure 9 shows a very good correlation between the sedimentation diameter determined from the settling experiments and the maximum length of the shells. It is of the form $d_s = 0.019d_w + 1.14$, $r^2 = 0.89$. This shows that the settling behavior, which is used to determine the sedimentation diameter, is linearly related to size and that shells of all sizes are hydrodynamically similar. The slope of the line is shallow particularly in comparison with the littorinid data (Amos et al. 2000), implying that cockle shell size has relatively little effect on sediment diameter and that the submerged mass is largely balanced by the increased area of the shells.

It was noted that the shells always remained in bedload transport and never entered into saltation. The theoretical onset of saltation should occur when $W_s \approx 0.8U_*$ (Bagnold 1966). This condition was satisfied for all the shells and yet they never saltated. This is due to their large deviation from sphericity, and it's resulting divergence from the friction angle (ϕ) for a well-sorted sand of around 30° (Table 2). For a shell resting on a plane surface, flow velocity beneath the shell is zero and lift is dependant upon the velocity distribution over the top of the valve. Pressure sensor work completed by Olivera and Wood (1997) has shown that flow around relatively convex shells results in steep longitudinal gradients from high to low pressure at the front of the shell, lateral restriction of both the low-pressure area over the mid-rear part of the shell and of the frontal pressure gradient, and a sudden downstream shift of the separation point with increasing velocity when compared to flow around flat shells. This prevents the development of a large drag force and contributes to lift; a convex shell is more likely to be lifted off the bed than a flat one. The shell of the edible cockle is relatively flat compared to shells such as the littorinid (Amos et al. 2000). It has a low shape factor (SF) where $SF = d_{sh}/\sqrt{d_i d_{max}} < 0.4$, with d_{sh}, d_i, and d_{max} referring to the shortest, intermediate, and longest diameters of the shells, respectively.

The lift forces acting on the shells have been disregarded for this investigation as they are thought not to affect the shells. The implication is that the presence of the shells will always result in high erosion levels as they are constantly in contact with the bed.

In 1936, Shields produced a threshold plot for grain movement. It contains three distinct zones whose limits correspond with three flow regimes: up to $Re \sim 3$, smooth boundary flow; $3 < Re < 200$, transitional region; and $Re > 200$, the rough turbulent regime. The cockle valves settle within the rough turbulent (impact) range, and so according to Shields (1936) should have a Shields criterion, θ_c, between 0.03 and 0.06, where $\theta_c = \tau_c/(\rho_s - \rho)gd_s$ (Dyer 1986).

While the majority of the shells were found to have a Shields criterion less than 0.035, the range extends to 0.10. This deviation from Shields work is attributed to the deviation from sphericity of the bivalve valves.

Bed Erosion

At the point of shell motion there is an increase in the suspended sediment concentration within the water column. An increase in the buoyant weight (F_W) of the shell used increases the erosion rate (Fig. 10) and therefore the suspended sediment concentration. This supports the intuitive conclusion that the greater the mass the greater the momentum transfer to the bed. Perhaps of greater significance is the lack of any description

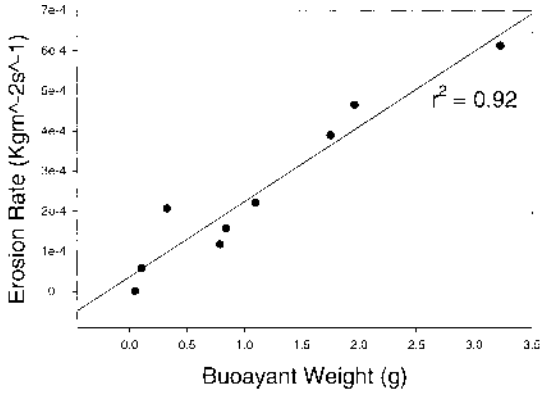

Fig. 10. The relationship between bed erosion rate and buoyant weight of disarticulated cockle shells inducing erosion. The erosion rate is linearly related to shell weight.

of bed properties in the equation, implying E is independent of bed character.

Implications in Nature

Although the laboratory experiments described here cannot be directly related to the natural environment due to the nature of the artificial clay bed, the processes at work can be assumed to occur to some extent wherever disarticulated cockle shells travel across cohesive sediments. If E is independent of bed character, then the laboratory experiments should be directly applicable to the field.

A trip to the Hythe salt marshes confirmed a large presence of disarticulated cockle shells on the beaches, salt marshes, and mud flats. Large volumes of shells were noted to accumulate at the base of cliffs in the mud flats. These cliffs have been noted to be retreating at a very rapid rate (French 2001) and field work is currently being undertaken to link the presence of the shells with this retreat. Large numbers of cockle shells are also found to accumulate in areas of the Lymington salt marshes and may be related to increases in erosion in this area. Track marks left in the bed by the cockle shells during the experiments are reminiscent of the furrows found in Southampton water, though on a much smaller scale. The rapidity of their formation may explain the rapid reformation of the furrows after activities such as dredging.

Comparison to Littorinids

The major difference between this work and the work by Amos et al. (2000) on littorinid-induced erosion was the absence of saltation and the sliding response of the cockle shells. The mechanisms controlling the erosion of the two beds are therefore different: one depending on the ballistic impacts of saltating littorinids to deliver momentum to the bed and the other on constant abrasion of the sediment surface without impact, although both are forms of solid-transmitted stress.

The differences in the shell behavior under flow, which depend on their geometry and size, are of prime importance to bed response. Littorinid shells require a greater drag force to lift them into saltation than to induce them to roll along the bed. This is explained by the fact that the littorinids have a much lower friction angle (20–30°) than the cockle shells (40–60°) and a greater concentration of mass. Both shell types cause significant bed erosion, even of highly cohesive beds that are resistant to fluid-transmitted stresses. The erosion rates of both sets of experiments are of the same order of magnitude implying that the momentum/energy transferred to the bed is approximately the same for both saltating littorinids and sliding cockles.

Comparison to *Ulva* sp.

Work has been carried out on the influence of mobile fragments of macroalgae of the species *Chondrus crispus* and *Fucellaria lumbricalis* on the erosion of prepared artificial beds also using the Mini Flume (Cozette 2000; Levy 2000). The results showed that mobile algae fragments significantly increased erosion rates and suspended sediment concentrations over that of the control experiments in which there was no apparent fluid-induced erosion of the bed, and that erosion rates and suspended sediment concentrations varied directly with respect to algal size and abundance. As with the cockle shells, motion begins by sliding, although unlike the cockle shells the algal fragments then roll, undergo a mixture of suspension and sliding, and finally move in continuous suspension. There was no standard saltation period for the fragments. It was found that algae contact time with the bed and the species of macro-algae significantly influenced the erosion rates of the artificial bed.

It was shown that slower moving algae (moving as bedload) had higher final suspended sediment concentration, as they transmitted more momentum to the bed. The cockle shells also yield a higher final suspended sediment concentration for the larger shells, which travel more slowly, as these also transmitted more energy to the bed. Maximum erosion rates were achieved during the sliding/rolling phase for the smaller pieces of algae, and during the mixed phase of suspension and sliding for the medium to large pieces. Suspended sediment concentrations ceased to increase and erosion rates declined to zero when the algae entered fully into suspension as no contact was made with the bed.

Summary and Conclusions

This study was undertaken to evaluate the potential effects of mobile shell valves of the bivalve *C. edulis,* the common cockle, on the erosion of dense, cohesive sediments. This was done as previous studies in Southampton Water had noted the abundance and mobility of mud furrows (Dyer 1970), which were linked with the presence of these bivalves. This study suggests that the furrows are not simply the products of increased turbulence, but are due to the abrasive effects caused by the shells when in motion by the tidal flows. The following were the major points of conclusion of our study.

The trends discussed above indicate that erosion is indirectly related to the flow velocity (Amos et al. 1997) because the flow velocity controls the behavior of shells travelling as bedload. An increase in shell size results in a reduction of overall shell velocity, but the shell speed increases with increasing flow velocity. The increase in shell size also increases the erosion rate and resulting suspended sediment concentration. This is due to an increase in the delivery of solid-transmitted stress to the bed.

The addition of a cockle shell to a bed of prepared cohesive clay results in the erosion of the bed. The larger the shell added, the greater the rate of erosion and the higher the levels of suspended sediment in the water column. The addition of the cockle shell is a significant mechanism for erosion on an otherwise stable bed.

Literature Cited

Allen, J. R. L. 1971. Mixing at turbidity current heads, and it's geological implications. *Journal of Sedimentary Petrology* 41:97–113.

Allen, J. R. L. 1985. Principles of Physical Sedimentology. Chapman and Hall, London.

Amos, C. L., G. R. Daborn, H. A. Christian, A. Atkinson, and A. Robertson. 1992. In situ erosion measurements on fine-grained sediments from the Bay of Fundy. *Marine Geology* 108: 175–196.

Amos, C. L., T. Feeney, T. F. Sutherland, and J. Luternauer. 1997. The stability of fine-grained sediments from the Fraser River Delta. *Estuarine, Coastal and Shelf Science* 45:507–524.

Amos, C. L., T. F. Sutherland, D. Cloutier, and S. Patterson. 2000. Corrasion of a remoulded cohesive bed by saltating littorinid shells. *Continental Shelf Research* 20:1291–1315.

Bagnold, R. A. 1936. The Physics of Blown Sand and Desert Dunes. Methuen & Company Limited, London.

Bagnold, R. A. 1966. The Physics of Sediment Transport by Wind and Water—A Collection of Hallmarked Papers. American Society of Civil Engineers, Washington.

Bishop, C. M. Skafel, and R. Nairn. 1992. Cohesive profile erosion by waves, p. 2976–2989. *In* B. L. Edge (ed.), Coastal Engineering, Proceedings of the Twenty-Third International Conference. American Society of Civil Engineers, New York.

Bitter, J. G. A. 1963. A study of erosion phenomena. *Wear* 6:5–21.

Cozette, P. M. F. 2000. Contribution of an Alga (*Ulva*) to the erosion of cohesive sediments: Towards the modelling of the phenomenon. M.S. Thesis, University of Southampton, UK.

Davidson-Arnott, R. G. B. and J. Ollerheads. 1995. Nearshore erosion on a cohesive shoreline. *Marine Geology* 122:349–365.

Dyer, K. R. 1970. Linear erosion furrows in Southampton water. *Nature* 225:56–58.

Dyer, K. R. 1986. Coastal and Estuarine Dynamics. John Wiley and Sons, Chichester.

French, P. W. 2001. Coastal Defences, Processes, Problems And Solutions. Routledge, London.

Granick, S. 1999. Soft matter in a tight spot. *Physics Today* July 1999, 26–31.

Houwing, E. 1999. Determination of the critical erosion threshold of cohesive sediments on interfacial mudflats along the Dutch Wadden Sea coast. *Estuarine, Coastal and Shelf Sciences* 49:545–555.

Houwing, E. and L. van Rijn. 1994. In situ determination of the critical bed-shear stress for erosion of cohesive sediments. *Coastal Engineering* 2:2058–2069.

Johansen, C., T. Larsen, and O. Petersen. 1997. Experiments on erosion of mud from the Danish Wadden Sea. Nearshore and Estuarine Cohesive Sediment Transport Conference INTERCOH 1994. Wallingford England. John Wiley & Sons, Chichester.

Kamphuis, J. W. 1990. Influence of sand or gravel on the erosion of cohesive sediment. *Journal of Hydraulic Research* 28:45–53.

Levy, A. 2000. The impact of saltating macrophytes on the erosion of a cohesive substrate. M.S. thesis. Acadia University, Wolfville, N.S., Canada.

Louis, H. and F. Pude. 2000. Application of a hand-controlled abrasive water jet system for dismantling of metal components. Proceeding of 15th Conference on Jetting Technology. British Hydraulics Research. Ronneby, Sweden.

Mehta, A. J., J. Lee, and B. A. Christensen. 1980. Fall velocity of shells as coastal sediment. *Journal of the Hydraulics Division, A.S.C.E.* 106:1727–1744.

Mehta, A. and K. Dyer. 1990. Cohesive sediment transport in estuarine and coastal waters in the sea. *Ocean Engineering Science* 9:815–839.

Murphy, P. J., A. M. Asce, and E. J. Aguire. 1985. Bed load or suspended load. *Journal of Hydraulic Engineering* 111:93–107.

Olivera, A. and W. Wood. 1997. Hydrodynamics of bivalve shell entrainment and transport. *Journal of Sedimentary Research* 67: 514–526.

Partheniades, E. 1986. A fundamental framework for cohesive sediment dynamics, p. 219–250. *In* A. J. Mehta, Estuarine Cohesive Sediment Dynamics. Springer-Verlag, Berlin.

Rice, M. A, B. B. Willets, and I. K. McEwan. 1996. Observations of collisions of saltating grains with a granular bed from high speed cine-film. *Sedimentology* 43:21–31.

Riddell, K. and T. Ishaq. 1994. Twenty years of beach monitoring along the south coast. 1994 MAFF Conference of River and Coastal Engineers, Ministry of Agriculture Fisheries and Food Flood and Coastal Defence Division, London.

Scarlatos, P. and A. Mehta. 1990. Some observations on erosion and entrainment of estuarine fluid muds. *Coastal and Estuarine Studies* 38:321–331.

Shields, A. 1936. Anwendung der Aehnlichkeitsmechanik und der Turbulenzforschung auf die Geschiebebewegung, Mitteilungen Preussischen Versuchsanstalt für Wasserbau und Schiffbau, Berlin. (Application of similarity principles and turbulence research to bed-load movement, English translation: W. M. Keck Laboratory of Hydraulics and Water Resources, California Institute of Technology, Report, 167. Pasadena, California.)

Skafel, M. G. 1995. Laboratory measurement of nearshore velocities and erosion of cohesive sediment (till) shorelines. *Coastal Engineering* 24:343–349.

Skafel, M. G. and C. T. Bishop. 1994. Flume experiments on

the erosion of till shores by waves. *Coastal Engineering* 23:329–348.

STRINGHAM, G. D, D. B. SIMONS, AND H. P. GUY. 1969, The behavior of large particles falling in quiescent liquids. Professional Paper. U.S. Geological Survey No 562C, Virginia.

SUTHERLAND, T. F., C. L. AMOS, AND J. GRANT. 1998. The erosion of biotic sediments: A comparison of methods. *Geological Society of London* 139:295–307.

SWAMEE, P. AND S. OJHA. 1991. Drag coefficient and fall velocity of nonspherical particles. *Journal of Hydraulic Engineering* 117: 660–667.

TEBBLE, N. 1966. British Bivalve Seashells. Alden Press, Osney Mead, Oxford.

WILLMARTH, W. N, N. E. HAWK, AND R. L. HARVEY. 1964. Steady and unsteady motions and wakes of freely falling discs. *Physical Fluids* 7:197–208.

WRIGHT, G. Z., S. HATIBOVIC-KOFMAN, D. W. MILLENAAR, AND I. BRAVERMAN. 1999. The safety and efficiency of treatment with air abrasion. *International Journal of Pediatric Dentistry* 9:1–7.

SOURCE OF UNPUBLISHED MATERIALS

FUNG, A. 1997. Calibration of flow field in Mini-Flume. Geological Survey of Canada, Atlantic Dartmouth, Nova Scotia.

Received for consideration, November 27, 2000
Accepted for publication, September 25, 2001